PHILOSOPHICAL TRANSACTIONS OF THE ROYAL SOCIETY A MATHEMATICAL, PHYSICAL & ENGINEERING SCIENCES

Ocean Models

A. E. Gill

Phil. Trans. R. Soc. Lond. A 1971 **270**, 391-413
doi: 10.1098/rsta.1971.0080

Phil. Trans. R. Soc. Lond. A. **270**, 391–413 (1971) [391]
Printed in Great Britain

Ocean models

By A. E. Gill
Department of Applied Mathematics and Theoretical Physics, University of Cambridge

[Plate 12]

Over the past twenty years or so, a good *qualitative* description of the ocean circulation has been built up through the use of two-dimensional wind-driven models. These correctly predict the position and sense of circulation of the major oceanic gyres, and explain the strong *western* boundary currents. However, the only *direct* measurements available for *quantitative* comparison with theory are those of the transport of the Gulf Stream. Observed values are considerably larger than those predicted by *linear* theory, but can be explained by *nonlinear* models.

Two-dimensional models have their shortcomings, however, because they take no account of vertical structure. They cannot properly model effects of nonlinearity, bottom topography, or of motions driven by thermohaline effects. They overlook important aspects of the circulation such as the equatorial undercurrent, and upwelling. Three-dimensional numerical models are designed to include these effects, and successfully reproduce, in a *qualitative* fashion, the major features of the ocean circulation. The models may be used for 'experiments' to find possible effects of changing parameters (such as the width and depth of Drake Passage), and to investigate the relative importance of different regions. With present-day computers, however, there are resolution and other problems which limit the degree to which the real ocean's parameters may be matched.

1. Two-dimensional models

In this talk, I would first like to review progress in the two-dimensional wind-driven ocean circulation models of the last twenty years or so. Then I want to discuss recent three-dimensional numerical models in more detail, giving some examples and discussing some of the problems associated with use of these models.

Let us consider now points on which circulation theories are reasonably successful in explaining features of the mean circulation of the ocean. One of the first successes may be attributed to the explanation of the east–west asymmetry of the ocean circulation. This is due to the so-called β effect which depends on the fact that the effect of the rotation of the Earth is dominant in ocean dynamics and the fact that the Earth's surface is curved. This means that currents are loath to cross circles of latitude unless forced to do so, and the appropriate expression of this is due to †Sverdrup (1947). †Stommel (1948) then pointed out the consequences for east–west asymmetry and showed that for a frictional model, currents are very much stronger on the western side of an ocean basin than on the east.

The next step forward was made by †Munk (1950) who used observed wind data to show that the position, number and sense of circulation of the major oceanic gyres are reproduced by the wind-driven circulation models. The Antarctic Circumpolar Current was once thought to be a misfit. Stommel (1957) discussed the problem qualitatively, and I (Gill 1968) was later able to show that conventional models give a satisfactory picture of this current if appropriate geographic features are properly modelled. Since then, computations have been done using wind data and actual ocean shapes which confirm the ability of these simple wind-driven models to reproduce the major oceanic gyres. I will show two examples. Figure 1 shows the result of a

† The papers of Sverdrup (1947), Stommel (1948) and Munk (1950) are reproduced in a book edited by Robinson (1963) and discussed in some detail by Stommel (1965).

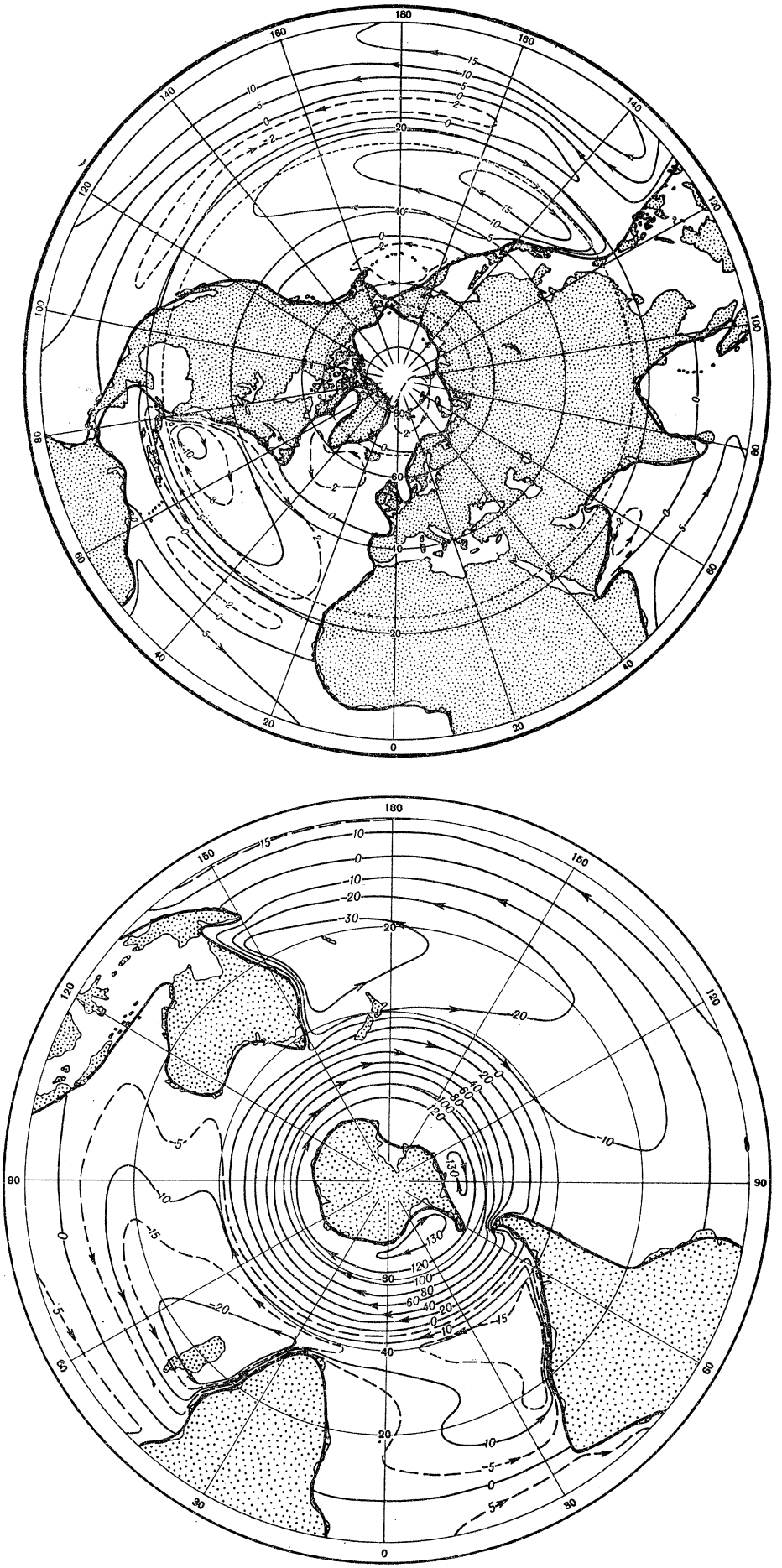

FIGURE 1. For legend see facing page.

PHILOSOPHICAL TRANSACTIONS OF THE ROYAL SOCIETY A MATHEMATICAL, PHYSICAL & ENGINEERING SCIENCES

computation by Ilyin, Kamenkovich, Zhugrina & Silkina (1969). Figure 2 shows the result of a computation by Takano (1969) using wind data from a different source and a different friction law but it basically shows the same gyres.

These results are very encouraging and lead one to believe that the major oceanic gyres are wind-driven. However, when one looks for quantitative agreement, the picture is less happy. Attempts to confirm Sverdrup's (1947) relation, which is assumed to hold in regions of weak currents, have failed (†Kendall 1970), but this could be due solely to the fact that we do not have direct measurements of velocities in these regions and calculations are based on the assumption

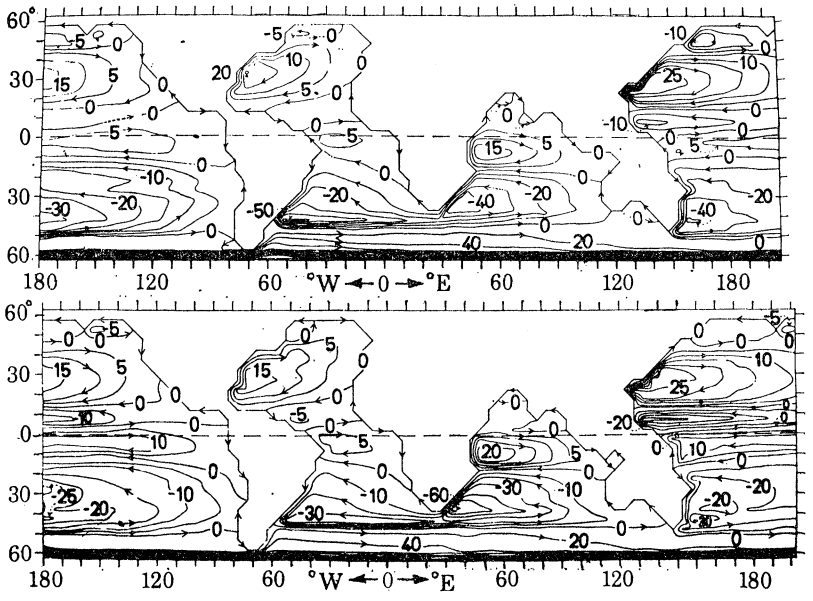

FIGURE 2. Transport stream function, ψ, for the world's oceans as computed by Takano (1969, Fig. 5), using a lateral friction model like that of Munk (1950). The value used for the lateral eddy viscosity was $10^4\,m^2\,s^{-1}$ ($10^8\,cm^2\,s^{-1}$) and the grid spacing was 5°. Values of ψ are given in units of $10^6\,m^3\,s^{-1}$. The upper figure was calculated using Hellerman's (1967, 1968) tables for the wind stress and the lower using Hidaka's (1958). The transport of the Antarctic circumpolar current is $196\times10^6\,m^3\,s^{-1}$ for the upper figure and $149\times10^6\,m^3\,s^{-1}$ for the lower figure.

that the deep water is not moving. Direct measurements have been made, however, in the Gulf Stream. According to the linear theories of Stommel (1948) and Munk (1950), the total mass transport of this current depends only on the field of wind stress in the ocean basin and so can be computed from wind data. Figure 3 shows the comparison of calculated and observed transports as a function of latitude. The values calculated from wind data are from a paper by Hellerman (1965, Table 3, column 7) and the observed values are from a recent paper by Knauss (1970). The observed transport is found to increase with latitude until the current flows eastward across

† Kendall's results for the North Pacific equatorial countercurrent were brought to my attention by Dr P. P. Niiler.

FIGURE 1. Transport stream function, ψ, for the world's oceans as computed by Ilyin, Kamenkovich, Zhugrina & Silkina (1969, Figs. 1 and 2). ψ is a solution of a finite-difference version of Stommel's (1948) equation

$$\epsilon\,\Delta\psi + 2\Omega a^{-2}\psi_\lambda = \mathrm{curl}_z\,\tau/\rho.$$

A stereographic projection was used with an average grid spacing of about 250 km. with the addition of a 'schematic viscosity'. $2\pi\Omega^{-1} = 1$ day, $\epsilon^{-1} = 15$ days, λ is longitude, a the Earth's radius, ρ density of sea water, and τ the wind stress calculated from mean pressure data (this gives a rather low estimate). Values of ψ are given in units equal to $0.4\times10^6\,m^3\,s^{-1}$.

the Atlantic. Munk (1950) was worried about a discrepancy between theory and observation of a factor of 2, but the recent information shows the discrepancy is much worse.

How can the discrepancy be accounted for? The answer seems to be provided by the consideration of nonlinear effects.† Figure 4 shows the transport as a function of latitude for a nonlinear

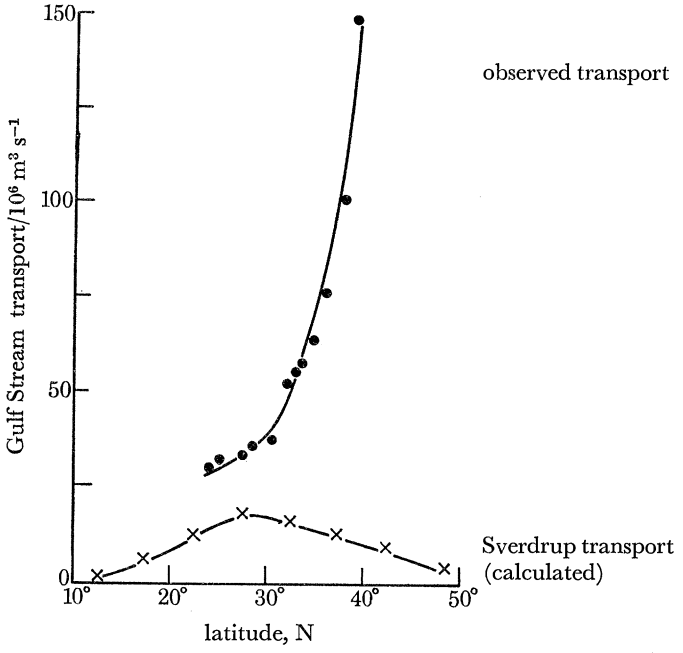

FIGURE 3. A comparison of the observed Gulf Stream transport (from Knauss 1970) and the transport according to linear theory, as computed from wind-stress data by Hellerman (1965, Table 3, column 7). Hellerman gives alternative values depending on the choice of drag coefficient. Those shown correspond to 'Derwent Hunter' data, which is the choice most consistent with recent evidence (see Hicks & Dyer 1970; Miyake *et al.* 1970; Smith 1970).

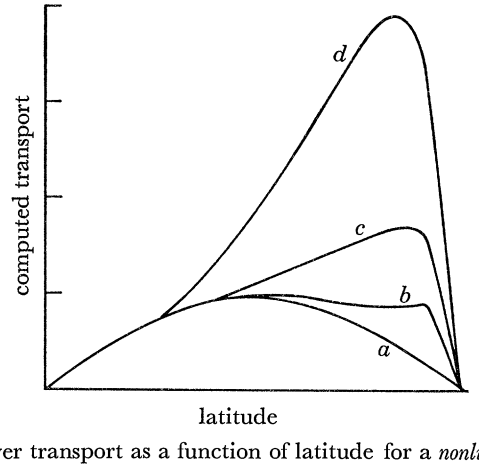

FIGURE 4. Western boundary-layer transport as a function of latitude for a *nonlinear* circulation model, with the friction decreasing successively from case *a* to case *d*. The values are taken from Veronis (1966) who computed solutions of the equation

$$\epsilon\Delta\psi + R\frac{\partial(\psi, \Delta\psi)}{\partial(x, y)} + \psi_x = \mathrm{curl}_z \tau.$$

In each case $R^{\frac{1}{2}}$ is 0.1 or 0.11 and the values of ϵ are as follows: *a*, linear case, $\epsilon > R^{\frac{1}{2}}$ (from Veronis, Fig. 4); *b*, $\epsilon = 0.05$ (from Veronis Fig. 7); *c*, $\epsilon = 0.025$ (from Veronis Fig. 8); *d*, $\epsilon = 0.018$ (from Veronis Fig. 9).

† *Note added in proof*: As a result of recent numerical experiments, W. R. Holland (private communication) has now suggested an alternative explanation which involves thermohaline effects and bottom topography.

model of Veronis (1966) for a series of cases in which the friction is successively reduced. The reduction of friction makes the variation of transport more and more like that observed and Niiler (1966) has shown that, for the type of friction used in the model, the maximum transport

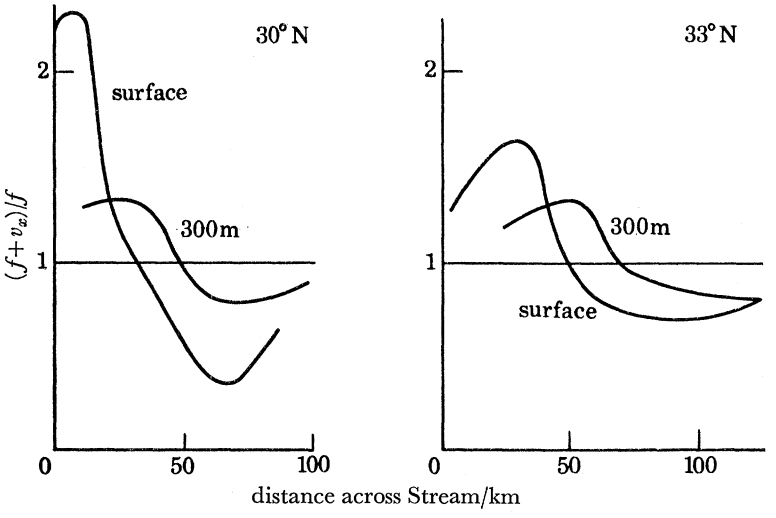

FIGURE 5. Ratio of the vertical component, $f+v_x$, of total vorticity, to the vertical component, f, of planetary vorticity as calculated from fig. 3(*b*) of Richardson, Schmitz & Niiler (1969) for two sections across the Gulf Stream. $f = 2\Omega \sin\phi$ where $2\pi\Omega^{-1} = 1$ day and ϕ is the latitude, and v_x is the cross-stream derivative of downstream velocity.

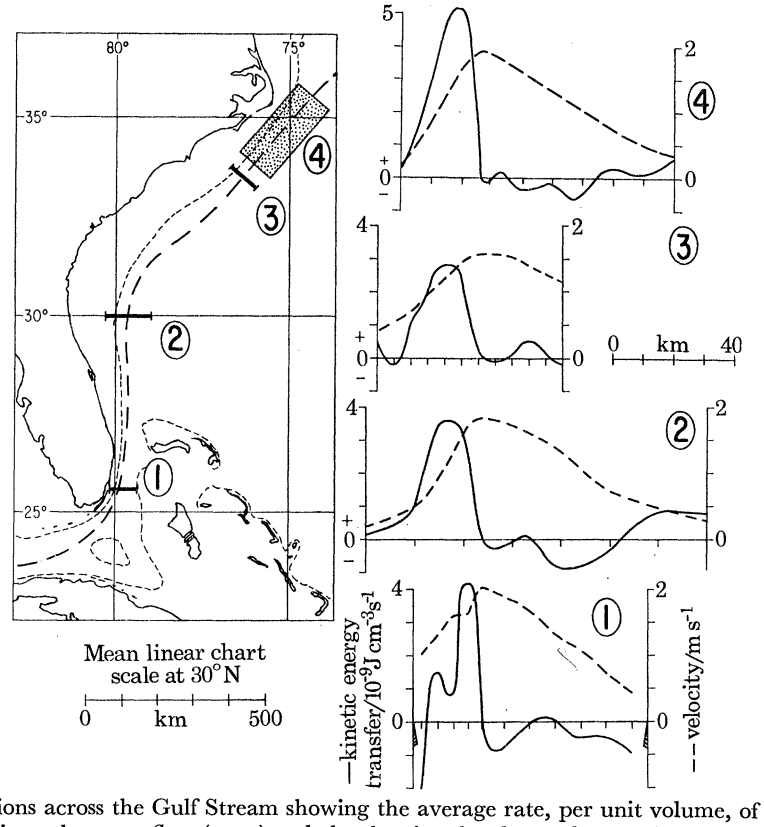

FIGURE 6. Four sections across the Gulf Stream showing the average rate, per unit volume, of transfer of kinetic energy *from* eddies *to* the mean flow (——) and also showing the observed mean downstream velocity (– – – –). This diagram is taken from Webster (1965, Fig. 1).

increases indefinitely as the friction parameter goes to zero. For lateral friction, a similar effect is found although a steady state is not always achieved (see Bryan 1963). The handling of nonlinear terms in the two-dimensional models of Veronis and Bryan is only strictly valid when the velocity is independent of depth, but similar effects are found in baroclinic models (see, for example, Bryan & Cox 1968*a*, Figs. 8*a*, 9). There is no doubt that the Gulf Stream itself is strongly nonlinear. A measure of nonlinearity is the ratio of the vertical component, $f+v_x$, of total vorticity to the vertical component, f, of planetary vorticity. Linear dynamics correspond to a value of this ratio of unity.

Figure 5 shows the large observed departures from this value. The values are calculated from diagrams in a paper by Richardson, Schmitz & Niiler (1969). In fact Morgan (1956) and Charney (1955) have produced good models of the southern portion of the Gulf Stream which ignore friction altogether. (These models are discussed by Stommel 1965, chapter 8).

A sad feature of the nonlinear models is that the value of the maximum transport depends on friction, and appropriate ways to treat or parameterize friction are not known. In fact the only information we have on friction is rather disturbing. Figure 6 from Webster (1965) shows that energy is being transferred from eddies to the mean current on the inshore edge of the Stream corresponding to a negative eddy viscosity! More recent observations of Schmitz & Niiler (1969) show the same feature. Ozmidov, Belyayev & Yampol'skiy (1970), using observations of currents in a polygonal array of meters in the Indian Ocean, calculated that energy was transferred from eddies to the mean flow near the surface, but not lower down. However, their results indicated a strong dependence on the period over which averages were taken.

(As a final example of a nonlinear computation part of a cine film made by Dr J. O'Brien at the National Center for Atmospheric Research, Boulder, Colorado was shown. This showed the establishment of currents in the North Pacific starting with a state of rest and then applying a wind stress field as calculated from data by Hellerman (1967, 1968).

2. Vertical structure

The theories I have discussed so far are two-dimensional, and aim to calculate the vertical integrals of the horizontal velocity components as functions of latitude and longitude. They say nothing about the way currents vary with depth. These theories fail to explain the equatorial undercurrent which was in fact rediscovered (see, for example, Matthäus 1969) after the wind driven models of Munk and Stommel had been put forward. These models show no current which particularly favours the equator and the undercurrent can only be understood by means of models which take account of variations with depth. The reason for the existence of the undercurrent can satisfactorily be explained by homogeneous† ocean models (Stommel 1960; Charney 1960; Robinson 1966; Gill 1971) and several have been proposed, the main differences being in the nature of the friction process involved. The reason for the existence of the undercurrent is illustrated in figure 7. The wind force on the surface is balanced by a difference in the forces due to the pressure on the coasts and the two ends of the current. Such pressure differences exist at other latitudes but are balanced by Coriolis forces. At the equator the Coriolis force vanishes, and so a direct down-gradient flow is produced. I have suggested (Gill 1971) a model in which lateral

† The models are homogeneous only in the sense that the region where currents are calculated is homogeneous. However, the lower boundary of this region is usually regarded as being the thermocline, rather than the ocean floor.

FIGURE 9. Experimental results of J. W. Elder (private communication) showing the effect of variation of β on currents through a model Drake Passage, which is at the top right of each picture. A thin layer (about 1 cm) of fluid is driven clockwise by an impellar which is seen (at the bottom of each picture). The β effect is provided by the free surface curvature which is produced by the rotation, and increases from (*a*) to (*c*). As β increases, so does the asymmetry of the motion through the gap, a western boundary current (corresponding to the Falkland current) being well-established in case (*c*).

(*Facing p.* 397)

PHILOSOPHICAL TRANSACTIONS OF THE ROYAL SOCIETY A MATHEMATICAL, PHYSICAL & ENGINEERING SCIENCES

friction is important. This has the nice property that the transport of the undercurrent is independent of the friction parameter and is given by the simple expression

$$\text{mass transport of undercurrent} = \pi\tau/\beta,$$

where τ is the wind stress and $\beta = 2\Omega/a$ where Ω is the angular velocity of the Earth and a its radius. This underestimates the transport by a factor of 4 or 5 but McKee (1970) has shown that the nonlinear effects can account for such a discrepancy. As with the Gulf Stream, measurements show the importance of nonlinear effects (Knauss 1966).

The other notable feature of three-dimensional constant density models is the existence of upwelling or downwelling zones around the edge. These have been studied by Hidaka (1954) and

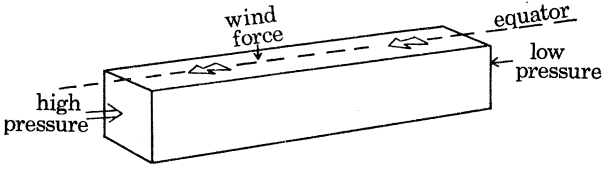

FIGURE 7. A sketch showing how the equatorial undercurrent is driven. At the equator, the force of the wind on the surface is balanced by the difference in the pressure-forces on the two ends. The undercurrent is directly driven by the resulting pressure gradient.

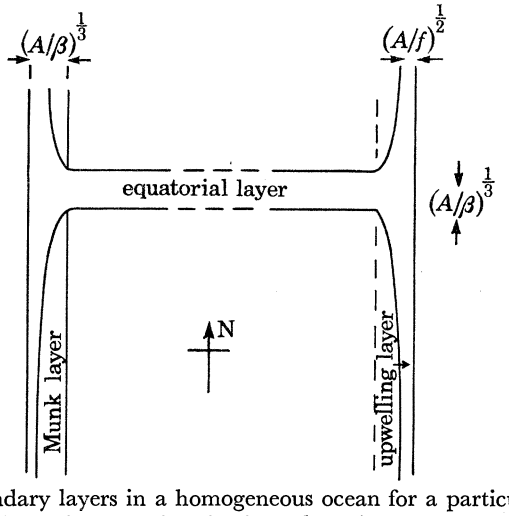

FIGURE 8. Arrangement of boundary layers in a homogeneous ocean for a particular parameter range. Inertial effects are neglected, the hydrostatic approximation is made and the bottom stress is zero. Symbols used are A, the lateral eddy viscosity, $f = 2\Omega\sin\phi$ and $\beta = 2\Omega a^{-1}\cos\phi$ where $2\pi\Omega^{-1} = 1$ day, a is the Earth's radius and ϕ is the latitude. The western boundary layer was discussed by Munk (1950), the upwelling layers by Hidaka (1954) and Pedlosky (1968), and the equatorial layer by Gill (1971). A western boundary layer, upwelling layers and an equatorial layer (or layers) are found for other parameter ranges, but details vary from case to case.

Pedlosky (1968). The upwelling is forced by the driving away by the wind of a surface layer from the coast, according to the theory of Ekman (1905). If a model like Pedlosky's is extended to the equatorial region, the arrangement of boundary layers is as shown in figure 8.

In discussing homogeneous models I should also say something about laboratory models such as those of von Arx (1952), Stommel, Arons & Faller (1958), Beardsley (1969), Baker & Robinson (1969) or Baker (1971). An example (J. W. Elder, private communication) which illustrates the role of the β effect is shown in figure 9, plate 12, the geometry of the situation having been designed to model the area around the southern tip of South America. However, laboratory

PHILOSOPHICAL TRANSACTIONS OF THE ROYAL SOCIETY A MATHEMATICAL, PHYSICAL & ENGINEERING SCIENCES

models have so far not played a fundamental role in the advance of our knowledge but have tended to confirm or demonstrate ideas already developed theoretically.

The homogeneous ocean models are helpful, but one could hardly call a model complete that does not take some account of stratification, or of the driving forces due to buoyancy fluxes across the ocean's surface. Some simple models indicate what may be the most important effects. First, two-layer models of the wind-driven circulation (see Stommel 1965) suggest that wind driven currents are mainly confined to the upper layers. Secondly, a useful picture of the deep water has been put forward by Stommel (1958) (see also Stommel & Arons 1959, 1960), the circulation being associated with localized sinking at high latitudes and upward motion in the remainder of the ocean. The upward motion implies vortex stretching in the deep water which in turn requires poleward flow except in narrow western boundary layers. Observations (see Warren & Voorhis 1970; Warren 1971) confirm the western intensification of the deep flow and show that the transport is in the predicted direction. These currents have considerable significance as the first currents whose existence was predicted by theory before they were actually observed. Thirdly, we have the thermocline models, which will be discussed by Welander (1971) in the following paper.

3. Three-dimensional numerical models

My discussion of three-dimensional numerical models will almost entirely be confined to results obtained by Dr K. Bryan and his co-workers at Princeton.† The models are set up as follows. First an array of grid points is specified throughout the model ocean with typically 20–30 grid points in each horizontal direction and 6 to 20 points in the vertical. Finite difference equations are set up to calculate values of the velocity, temperature, and possibly salinity at the different points using finite difference approximations to the equations of motion. The physical approximations normally made are:

(*a*) The hydrostatic approximation.

(*b*) Neglect of the Coriolis force associated with the vertical velocity component.

(*c*) Eddy viscosity and eddy diffusivity coefficients are introduced in the usual way. Constant values have mainly been used, with different values for horizontal and vertical mixing processes.

(*d*) The representation of convective overturning effects by a process which vertically mixes any part of a fluid column which is tending to become statically unstable.

Various configurations of boundaries and of bottom topography have been used. The wind stress is specified at the surface and so is the temperature (and possibly salinity) of the surface layer.

Now there are certain problems of resolution which lead to compromises in the choice of parameters and the computer time for each calculation is so large that only limited studies of the effects of changing parameters can be made. This means that evaluation of results tends to be more qualitative than quantitative.

3.1. *Ability of models to reproduce observed features*

As far as qualitative features are concerned, the models do rather well.

First of all the basic thermocline structure is reproduced, and all the deep water is cold. An example of a computed meridional section of specific volume anomaly is shown in figure 10, with an observed meridional section for comparison. One can also see the downward bowing of isolines in the subtropical gyre in each picture.

† The pioneering work on three-dimensional numerical ocean models was done by Sarkisyan (1966).

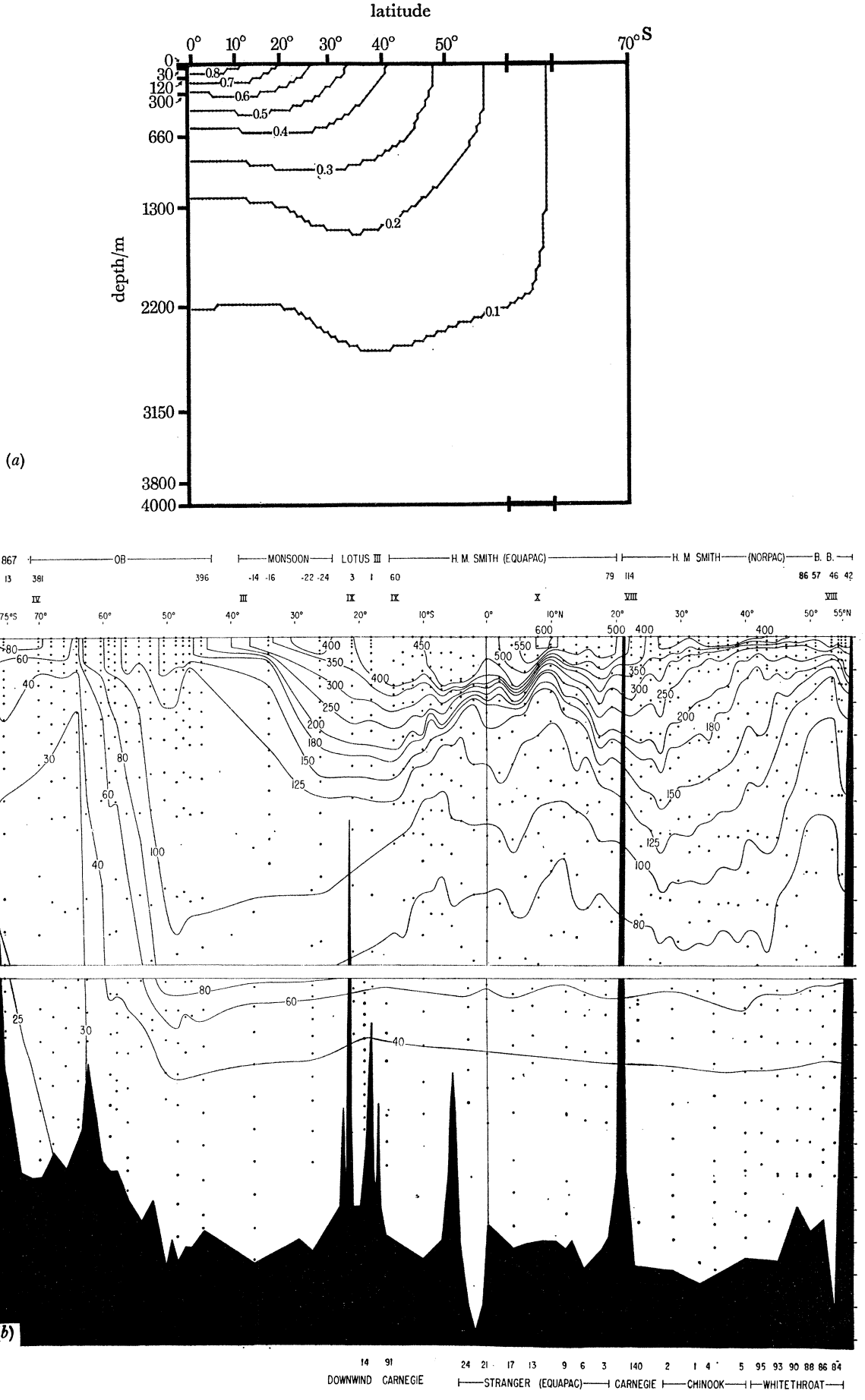

FIGURE 10. Comparison of (*a*) computed and (*b*) observed meridional sections of specific volume anomaly. (*a*) is the section down the centre of the basin for case 15-I of Gill & Bryan (1971) in non-dimensional units, while (*b*) is a mid-Pacific section showing thermosteric anomaly in centilitres per ton (from Reid 1965).

PHILOSOPHICAL TRANSACTIONS OF THE ROYAL SOCIETY A MATHEMATICAL, PHYSICAL & ENGINEERING SCIENCES

Secondly the strongest currents are found near the surface, as observed.

Thirdly the models seem to be able to reproduce the main currents in the right places. For example, figure 11 shows a computed section across a model Gulf Stream compared with an observed section. This picture is taken from Bryan & Cox (1968*a*).

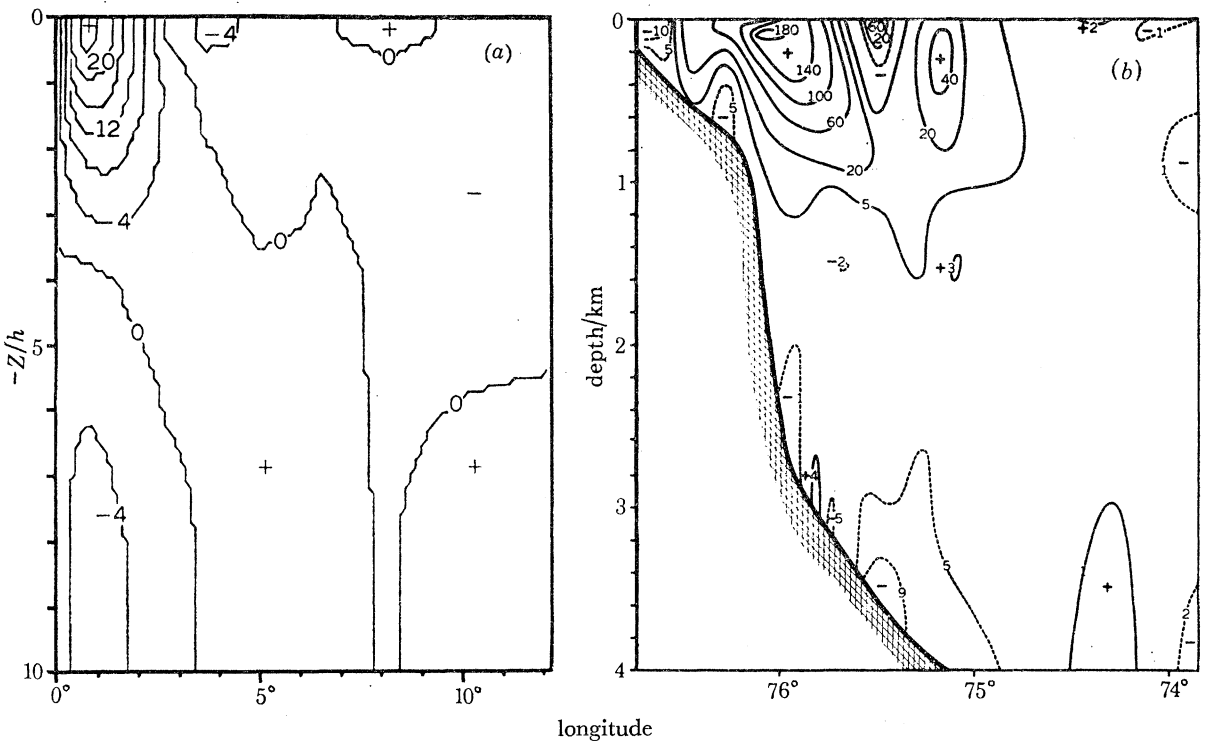

FIGURE 11. (*a*) Computed western boundary current at 28° N given in non-dimensional units. (*b*) An observed profile of the Gulf Stream off Cape Hatteras given by Swallow & Worthington (1961). Units are centimetres per second. (Fig. 18, Bryan & Cox 1968*a*.)

Another example is the equatorial undercurrent. Figure 12*a* shows contours of eastward velocity from a model of W. R. Holland (private communication). The current is in the right place and in the right direction but is rather weak because of the choice of a rather large eddy viscosity. The corresponding temperature section shows the rather characteristic bowing of the isotherms. Another example is the reproduction of the Somali current in the Indian Ocean model of Cox (1970) in which seasonal variations were studied.

3.2. *Possibility of analysing balances of terms*

The models may be helpful in a variety of ways. From one point of view they may be regarded as an attempt to reproduce features of the ocean circulation in a numerical model. From another, they may be viewed as a means to obtaining an understanding of the dynamics of various ocean currents. The dynamics of the models may be examined by investigating balances of terms in various equations, or balances of forces on various blocks of ocean, etc. Examples of this approach may be found in Bryan & Cox (1968*b*).

Figures 13 and 14 illustrate how information about balances of terms may be conveniently displayed. From figure 13*a*, for instance, it is clear that advection of vorticity is important in the model in the upper layers. The existence of a western boundary layer in the deep water is clear

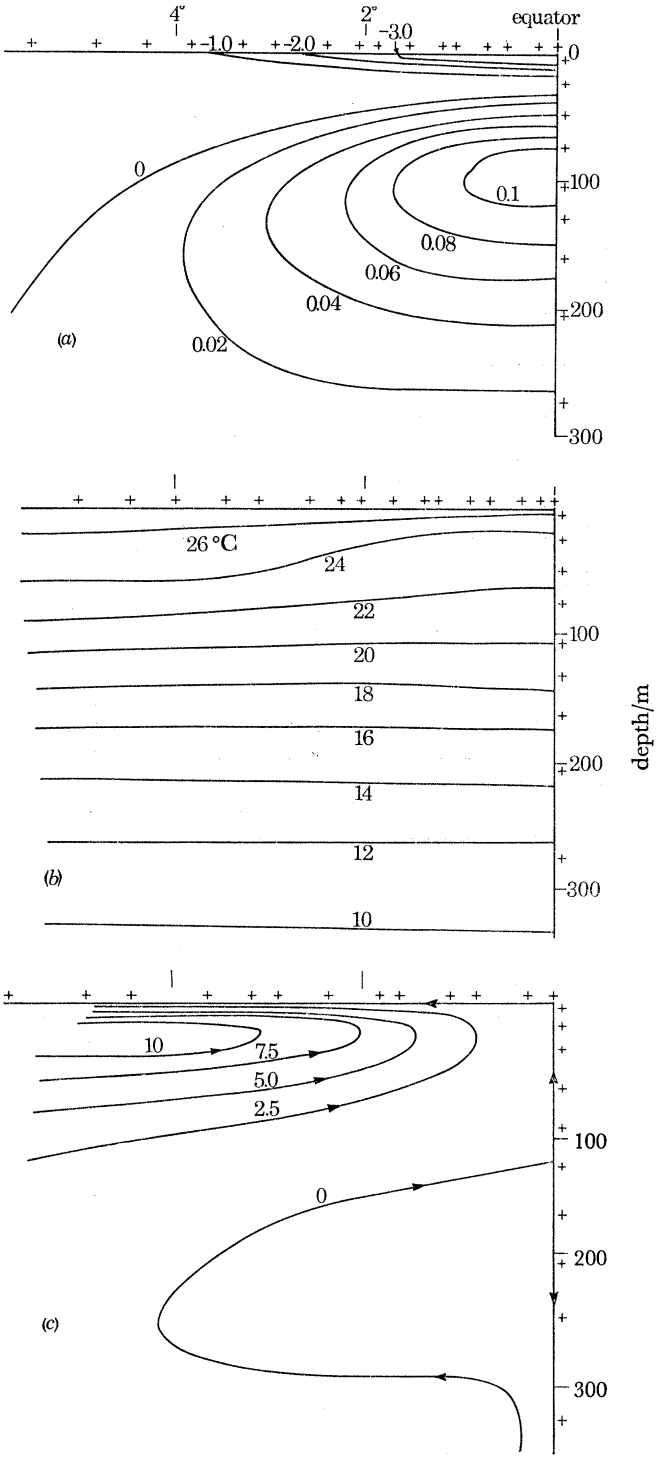

FIGURE 12. Some preliminary results of W. R. Holland (private communication) for the equatorial region showing meridional sections with (*a*) contours of eastward velocity in m s^{-1}, (*b*) temperatures in °C, and (*c*) contours of meridional transport stream function, in units of 10^6 m^3 s^{-1}.

A model like that of Bryan (1969) has been used with the following values of the parameters.

$$A_M = 5\times10^4\ \mathrm{m^2\,s^{-1}},\quad A_H = 5\times10^3\ \mathrm{m^2\,s^{-1}},\quad \kappa = 10^{-4}\ \mathrm{m^2\,s^{-1}},\quad \nu = 10^{-3}\ \mathrm{m^2\,s^{-1}}.$$

The wind-stress distribution is a zonal average of Hellerman's (1967, 1968) wind data. The wind stress at the equator was 0.029 N m^{-2} (0.29 dyn cm^{-2}) westward. The position of the grid points is marked. The computations were made for the northern half of a basin 4 km deep occupying 20° of latitude each side of the equator and 45° of longitude. Symmetry was assumed about the equator. At the surface, wind stress, temperature and salinity were specified. At the northern boundary, temperature and salinity were specified and the vertically integrated northward velocity was set at zero.

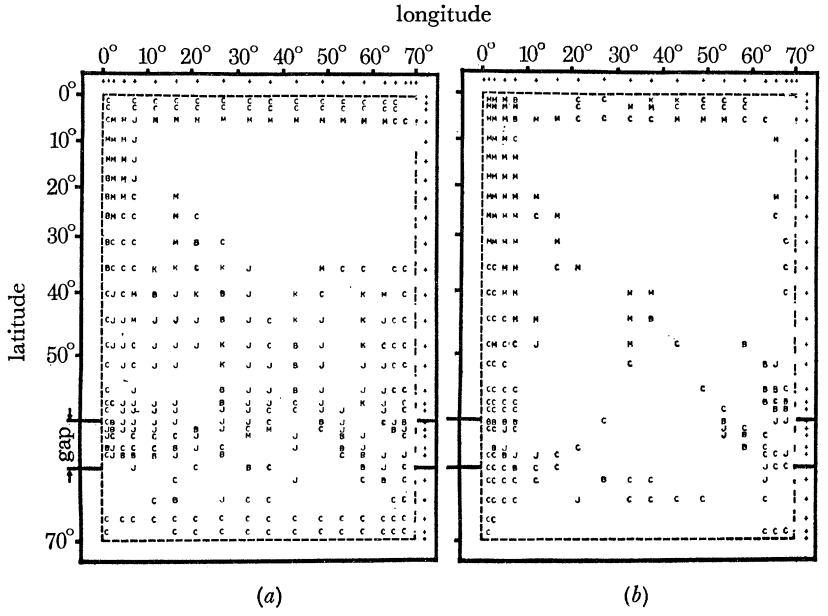

FIGURE 13. The balance of terms in the vertical component of the vorticity equation at each grid point at (*a*) a depth of 300 m, (*b*) a depth of 3000 m (corresponding to levels $k = 3, 7$ respectively for case 15-I of Gill & Bryan 1971). The magnitude of each term in the vorticity balance has been calculated and the letter indicates the two terms of greatest magnitude according to the following scheme: B, lateral diffusion, nonlinear term; C, lateral diffusion, fw_z; M, lateral diffusion, βv; J, nonlinear term, fw_z; K, nonlinear term, βv. A blank indicates a balance between βv and fw_z. (The symbols β, v, f and w_z have the usual meanings.)

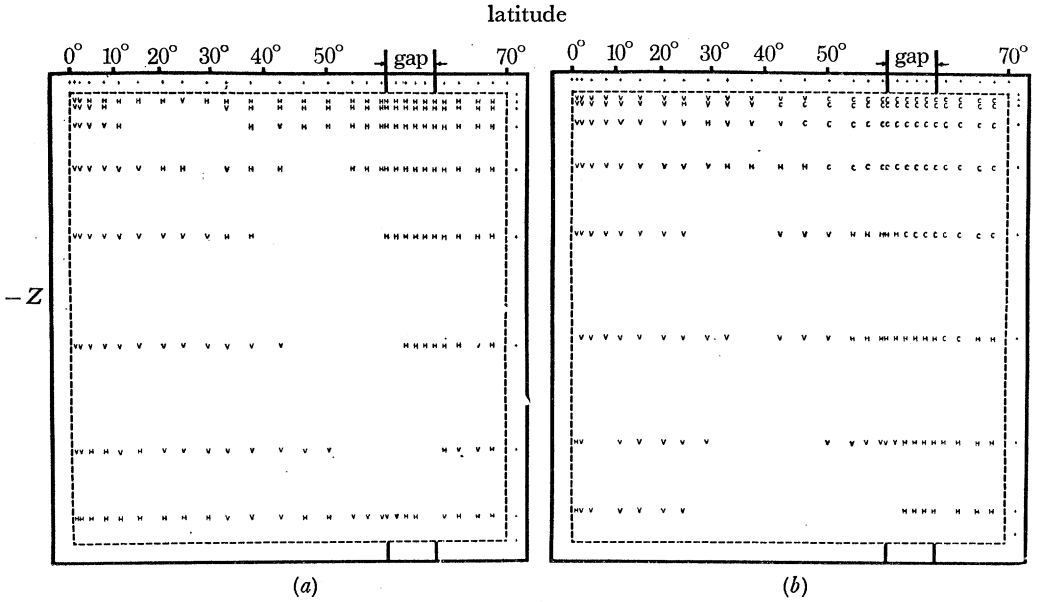

FIGURE 14. Balance of terms in the temperature equation for a mid-ocean meridional section (case 15-I of Gill & Bryan 1971). (*a*) The dominant *advection* term: H denotes that the horizontal advection term is larger than the vertical advection term, and V denotes that the vertical advection term, wT_z, is larger. A blank denotes that the advection terms are both larger than all the mixing terms, and therefore are in approximate balance with each other. (*b*) The dominant *mixing* term: the largest of these three terms is denoted by H, V or C where H denotes horizontal diffusion, V vertical diffusion and C the convective adjustment process. A blank denotes that two of the mixing terms are bigger than either advection term and so are in approximate balance. At most points, however, a mixing term balances an advection term, the exceptions being the points for which there is a blank in one of the diagrams.

PHILOSOPHICAL TRANSACTIONS OF THE ROYAL SOCIETY A MATHEMATICAL, PHYSICAL & ENGINEERING SCIENCES

from figure 13*b*. Figure 14 shows that, in the model, there is an approximate balance between vertical diffusion and vertical advection of heat in the deep water and in the tropics. Such a balance appears to be consistent with observation and has been found useful for estimating the rate of upwelling of deep water (Munk 1966).

3.3. *An investigation of possible geometric effects on the circulation*

Another use has been an investigation by Dr Bryan and myself of effects of geometry on the circulation in a model representing a southern hemisphere ocean. The three geometries used are shown in figure 15. Computations were made for each case using exactly the same parameters and

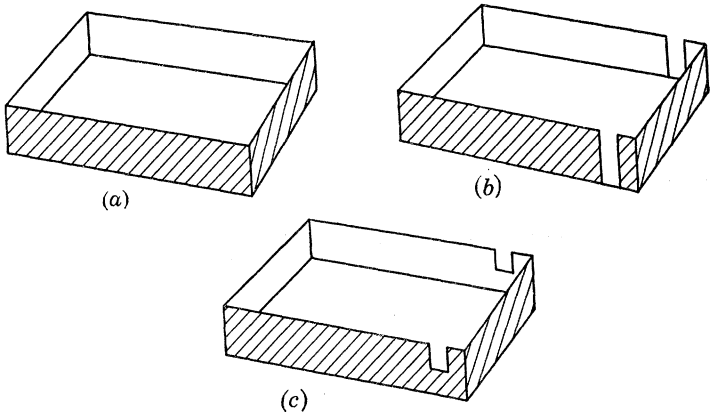

FIGURE 15. The three geometries used in a study by Gill & Bryan (1971): (*a*) a closed basin, (*b*) a basin with a deep gap representing Drake Passage, (*c*) a basin with a shallow gap. This model is designed to include the blocking effect on the deep water of the Scotia Ridge. When the gap is present, the water flowing out through the gap on one side of the basin is taken to be identical to the water flowing in the other side, that is, a periodicity condition is imposed at the gap.

exactly the same prescribed surface conditions. The first case represents a conventional closed-basin model. The second has a gap which is meant to represent Drake Passage and the ocean depth is constant. In the third case, the bottom half of the gap is blocked up, this representing the effect on the deep water of the Scotia Ridge which lies a little east of Drake Passage.

The effects of these simple changes of geometry are very striking. First, there is a strong effect on the meridional circulation, shown in figure 16. This shows meridional sections for the three cases. The function shown is a stream function for the transport obtained by integrating velocities from west to east. Figure 16*a* shows the circulation typically obtained in a closed basin. The integrated motion shows a narrow region of descending water at the polar boundary and rising over most of the remainder of the ocean. This circulation is largely thermally driven and is still found in the absence of wind stress (Bryan & Cox 1967). In the deep-gap case, this gyre is split into two so that now there is descending water north of the gap and upwelling south of the gap. The reason for this is the lack of an east–west pressure difference in the gap, and we feel this effect explains why Antarctic intermediate water is formed. In the shallow-gap case there are still two gyres. There is also a strong effect on the horizontal transports, as shown in figure 17. The striking effect here is the increase in the transport by a factor of 3 when the bottom half of the gap is closed. The increase is a thermally driven current due to a pressure difference set up across the barrier in the bottom half of the gap.

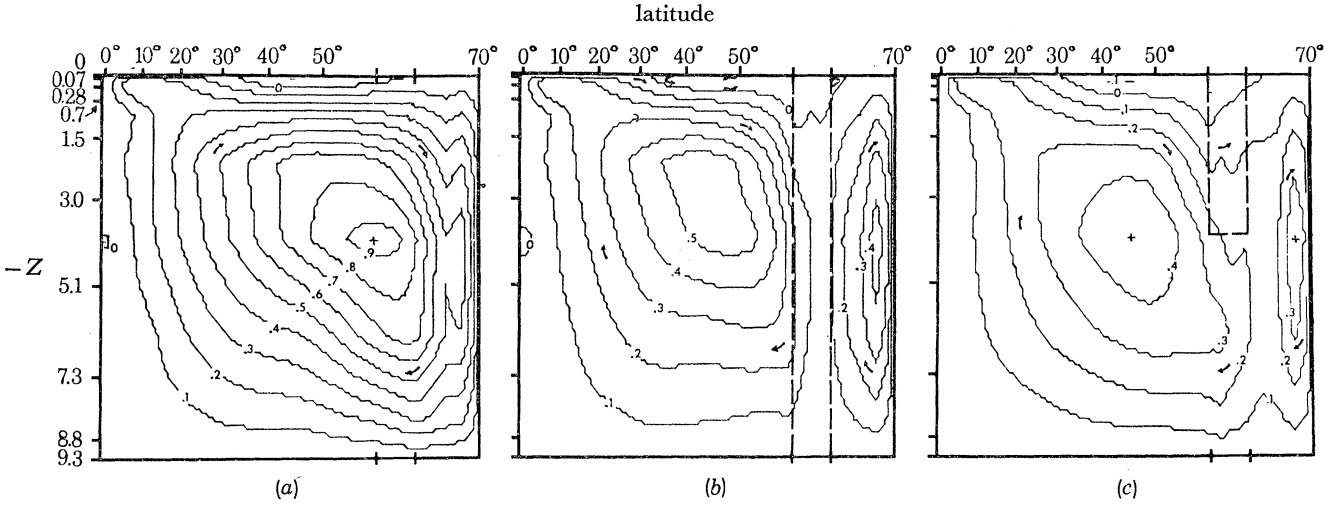

FIGURE 16. The meridional circulation for the three cases shown in figure 15, namely (*a*) closed basin, (*b*) deep gap and (*c*) shallow gap. The function plotted is the meridional transport stream function, $\psi^{(M)}$, defined by

$$\frac{\partial \psi^{(M)}}{\partial z} = -a\int_0^{\lambda_1} v\cos\phi\,\mathrm{d}\lambda, \quad \frac{1}{a}\frac{\partial \psi^{(M)}}{\partial \phi} = a\int_0^{\lambda_1} w\cos\phi\,\mathrm{d}\lambda,$$

where λ, ϕ, z are respectively longitude, latitude (positive northwards) and distance upwards, and u, v, w are the corresponding velocity components. a is the radius of the Earth and 0, λ_1 are the longitudes of the western and eastern walls respectively. Values of z and contours of $\psi^{(M)}$ are given in non-dimensional units (Gill & Bryan 1971).

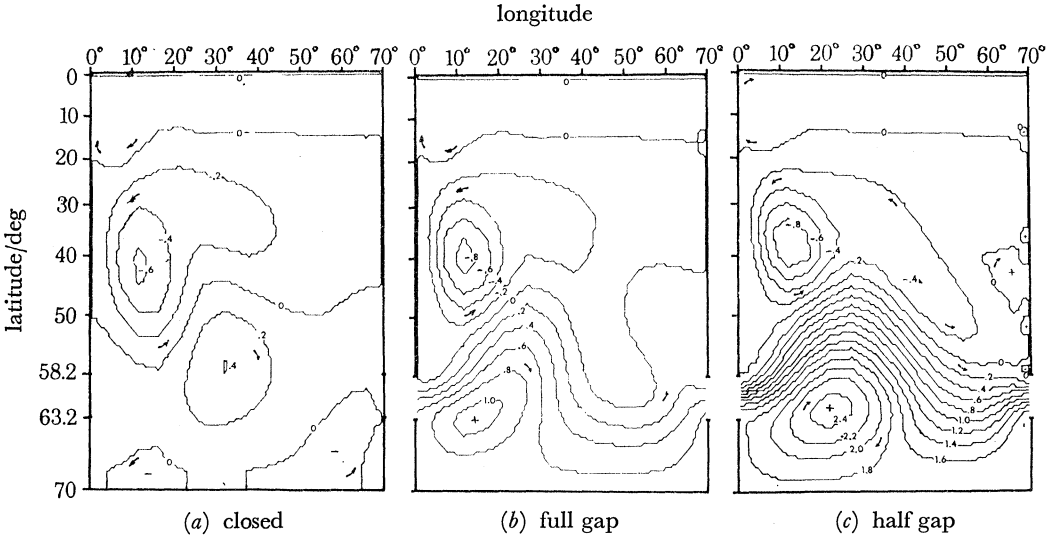

FIGURE 17. The horizontal circulation for the three cases shown in figure 15, namely (*a*) closed basin, (*b*) deep gap and (*c*) shallow gap. The stream function ψ is shown in non-dimensional units (Gill & Bryan 1971).

3.4. *Coastal upwelling and downwelling*

Another interesting effect found in models is the establishment of the Somali current in the Indian Ocean model of Cox (1970). The northern part of the current appears to be set up in direct response to the local winds which, because of proximity of the equator and their direction, produce a strong upwelling at the coast which results in the long-shore current. Figure 18 shows the upwelling and the tilts in the isotherms associated with the upwelling and associated geostrophically with the current.

The upwelling and downwelling regions are very striking features of the models and deserve a great deal of further study as phenomena in their own right. It is surprising how little attention has been given to them considering the economic importance of upwelling regions. The vertical

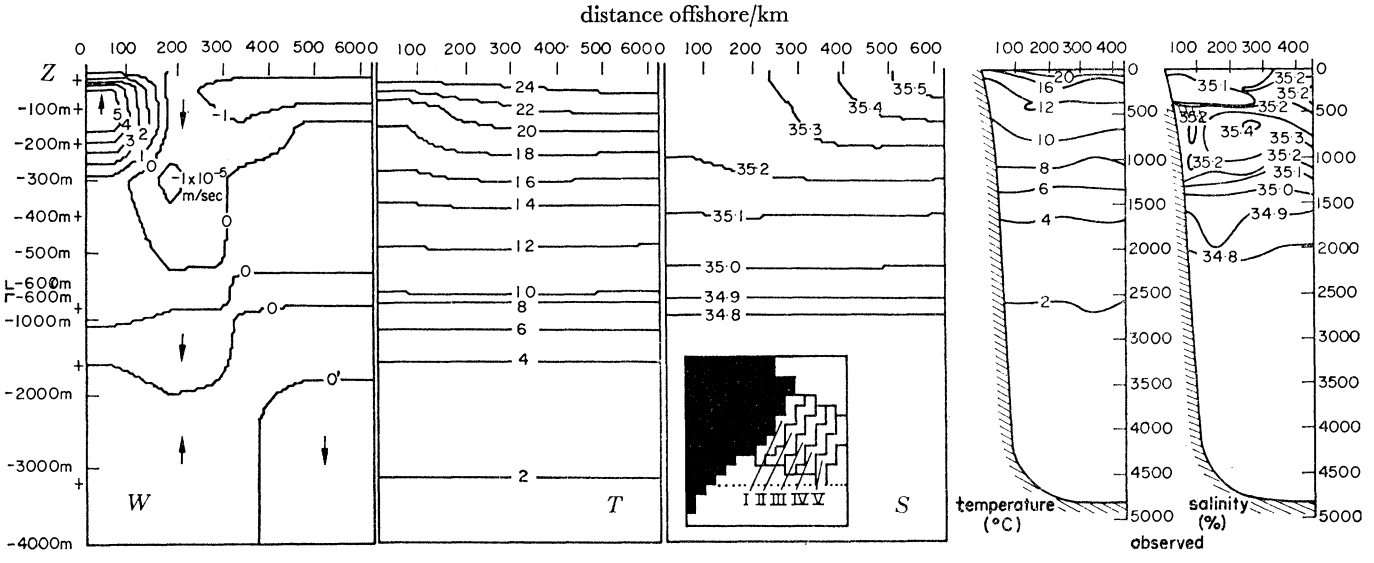

FIGURE 18. Results of a model showing coastal upwelling in relation to the Somali current (Cox 1970, fig. 13). The computed vertical velocity (W), temperature (T) and salinity (S) are shown, these being averaged over the summer within the five regions shown in the inset. The positions of grid points in the vertical are shown by crosses. Observed temperature and salinity profiles for August from Warren, Stommel & Swallow (1966) are shown for comparison.

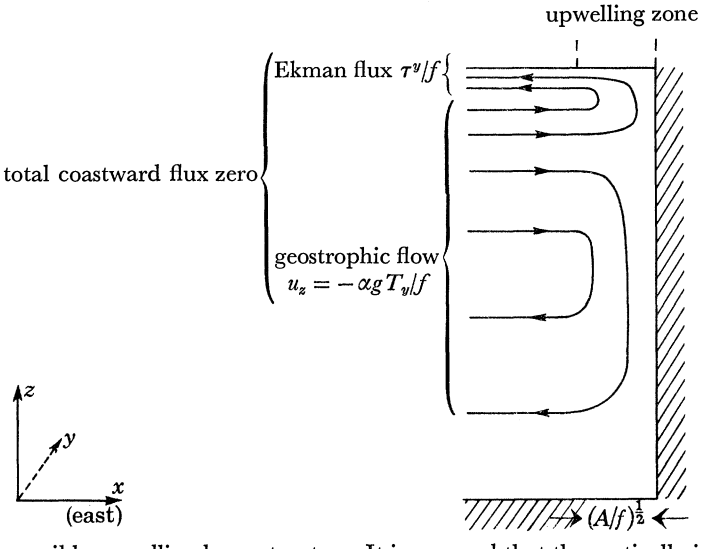

FIGURE 19. Sketch of a possible upwelling layer structure. It is assumed that the vertically integrated flow normal to the coast is zero, but that the upwelling redistributes the flow at different levels in order to preserve continuity.

velocities here are hundreds of times bigger than in the interior of the ocean. The sort of picture I have of these layers at the eastern boundaries of the *models* is indicated in figure 19, although these layers are not generally well resolved. The upwelling layer takes care not only of the Ekman flux at the surface, but redistributes the geostrophic velocity into the coast. Wooster & Reid (1963) have calculated the Ekman fluxes normal to the ocean's eastern boundaries to see how

well this correlates with indicators of upwelling such as reduced surface temperature. They did not, however, take account of the component of the geostrophic motion normal to the coast, although Wyrtki (1963) has done so for the region off Peru. A feature is that the density of a fluid element is changed while it is in the layer, and that is one reason for the difficulty in modelling them. Difficulties of resolution apply not only to models but to observation of these features. If the scale indicated is relevant, then scales of the order of 10 km or less are involved. That such small scales are observed is shown in figure 20 of the California undercurrent region (from Wooster & Jones 1970). Features with this scale have also been observed off the coast of Oregon (Smith, Pattullo & Lane 1966; Pak, Beardsley & Smith 1970).

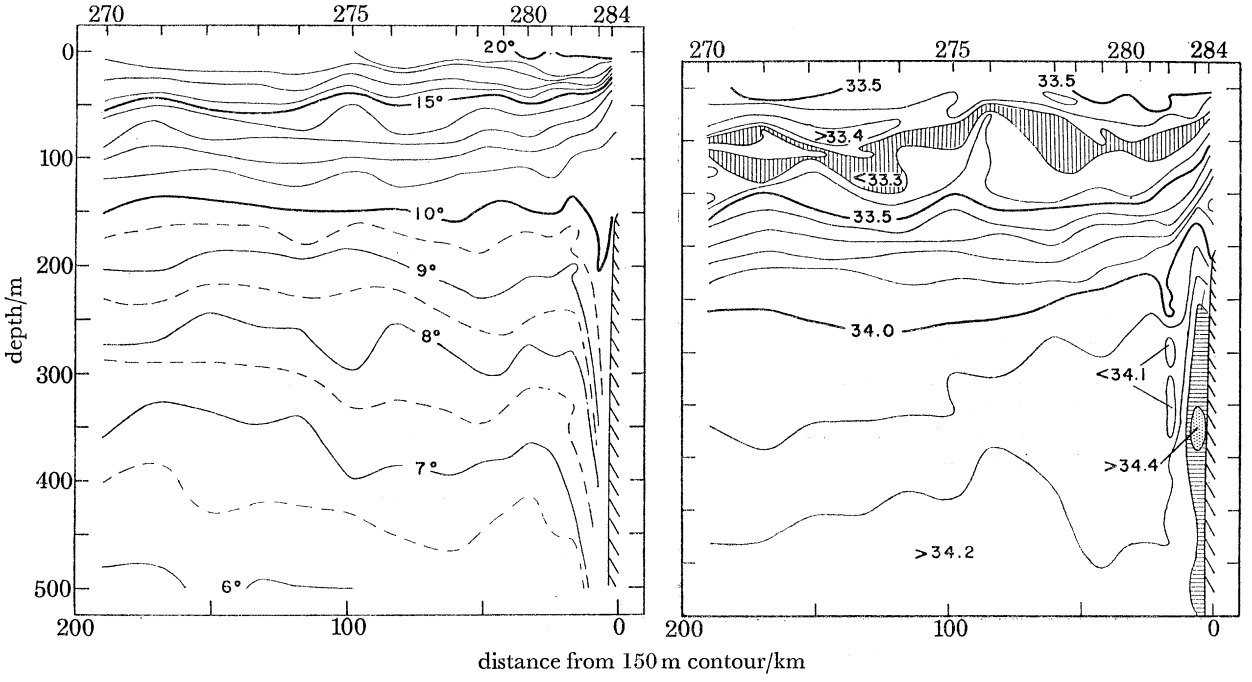

FIGURE 20. (*a*) Temperature and (*b*) salinity on a section normal to the coast of Baja California (30°–31° N) showing a thin upwelling region near the coast. Positions of stations are shown at the top (taken from Wooster & Jones 1970, figs. 9, 10).

The same sort of dynamics are appropriate to downwelling regions as well. Consider the section from the southwest Weddell Sea shown in figure 21. The station spacing is much too large to resolve the boundary layers which again could be on a scale as small as 10 km. There is particular interest in this region where Antarctic Bottom Water is being formed. Now, because of rotation effects, it is difficult to see how the rate of bottom water formation estimated from observations could be achieved purely as a result of buoyancy forces acting in the Weddell Sea. Cold water tends to run downhill only in narrow layers in which friction is important, and estimates of the buoyancy-driven flux in these layers give very small values. On the other hand, the wind can drive a sizeable Ekman flux towards the coast, forcing an equal amount of shelf water to flow down the continental slope. A research student, P. D. Killworth, is using a two-dimensional model designed to throw light both on the upwelling process and on the bottom water-formation process. He examines a meridional section across a zonal channel as shown in figure 22. The surface is cooled on the south side and warmed on the north side. The diagram illustrates the marked increase in the flow down the slope when the wind is blowing, and shows a

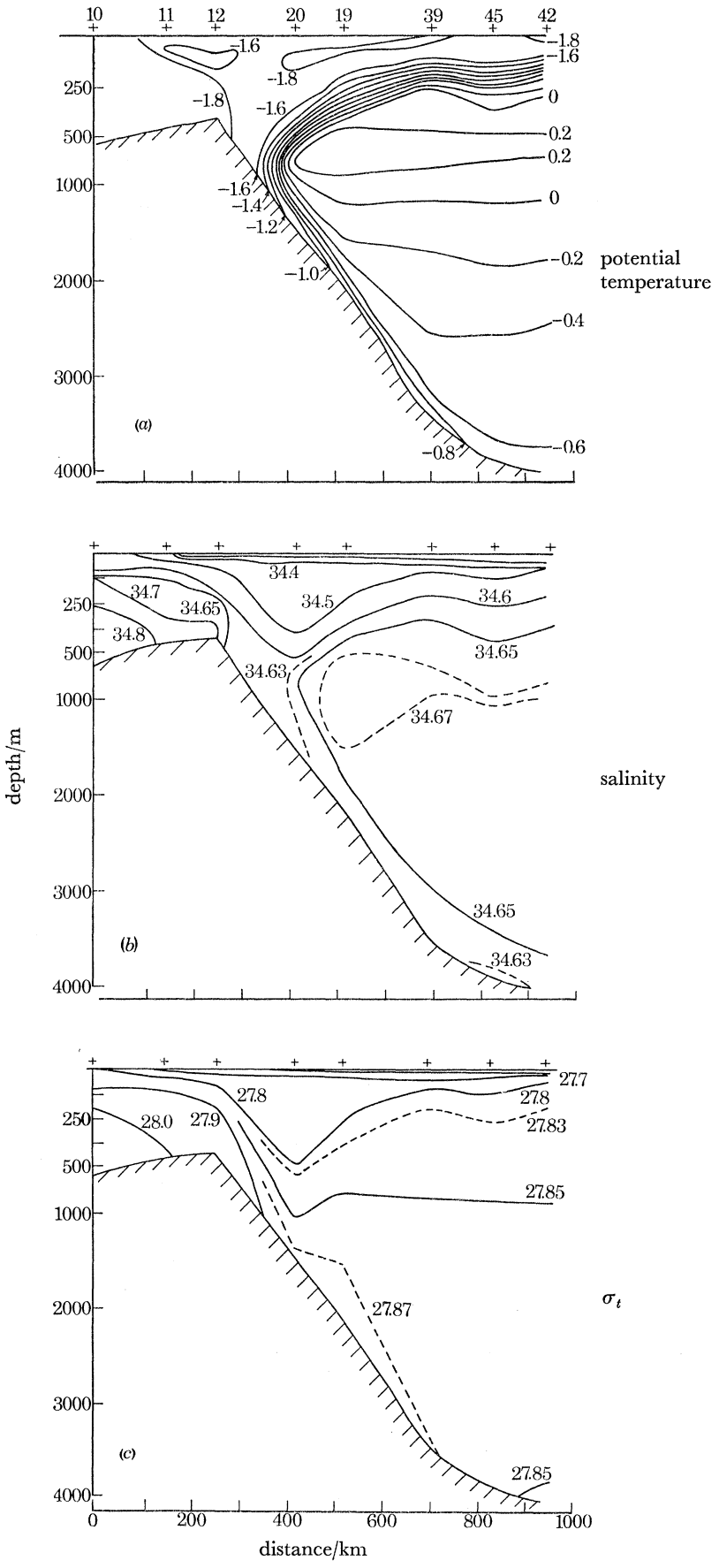

FIGURE 21. (*a*) Potential temperature (°C). (*b*) Salinity (‰), and (*c*) σ_t for a section in the southwest Weddell Sea running from 75° S, 60° W to 70° S, 40° W (approx.). Diagrams (*a*) and (*b*) were prepared by D. E. Moore (private communication) from data collected by U.S.C.G.C. *Glacier* during the International Weddell Sea Oceanographic Expedition, February to March 1968. Station positions are marked by numbered crosses. Note that the front near station 20 is not properly resolved, and that the exact position of the break in slope (shown at station 12) is not known.

PHILOSOPHICAL TRANSACTIONS OF THE ROYAL SOCIETY A MATHEMATICAL, PHYSICAL & ENGINEERING SCIENCES

more realistic density distribution (compare figures 21*c*, 22*a* (ii)). It is interesting to note also that the scales of the upwelling and downwelling layers are not easily discernible in the density fields.

To return to the three-dimensional models, I think their usefulness has been amply demonstrated. A project under way at the moment at Princeton is designed to calculate the velocity field in the ocean using the observed density field. (cf. Sarkisyan 1969; Sarkisyan & Pastukhov 1970). It may be considered a way of determining the level of no motion. This involves much less computer time than the full model as one does not have to wait for the density field to come

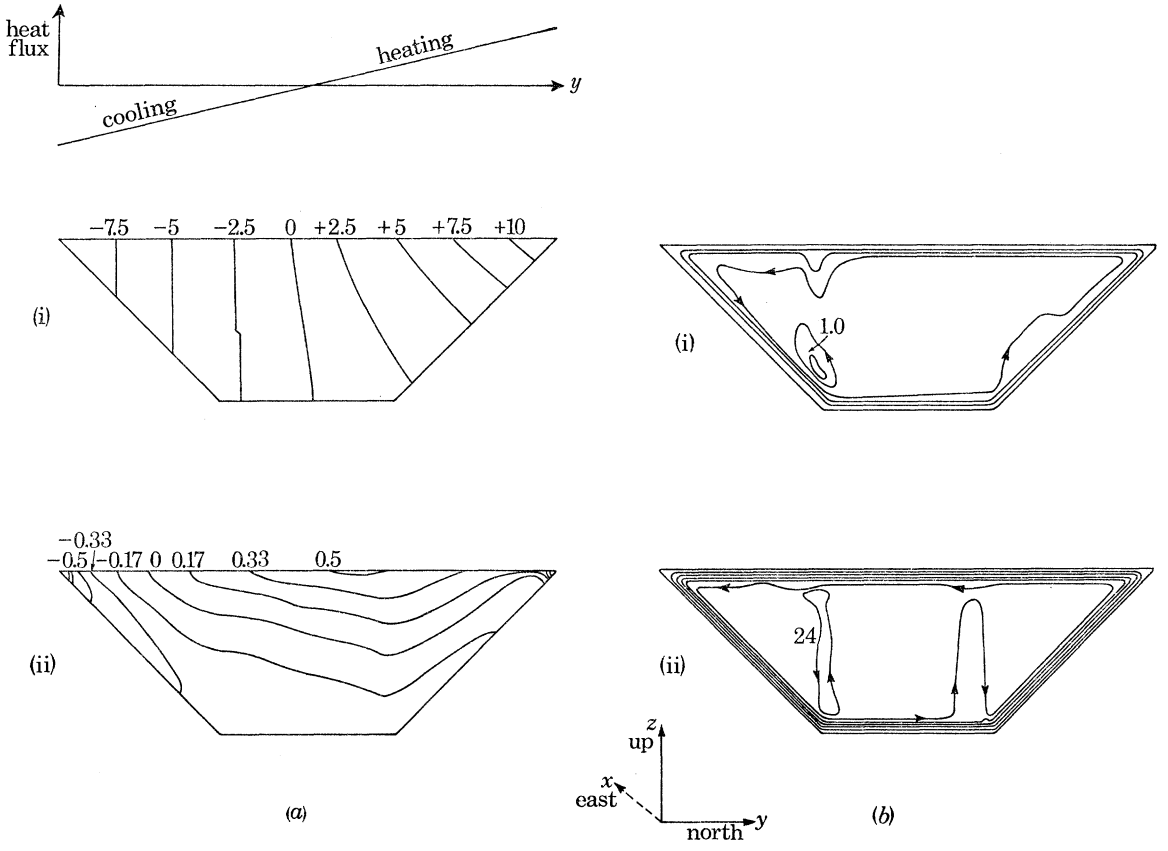

FIGURE 22. Numerical solution for a zonal channel with heating and cooling at the surface showing (*a*) isopycnals (non-dimensional units) and (*b*) the meridional circulation (contours in non-dimensional units of the meridional transport stream function). In case (i), the surface stress is zero; in case (ii), a uniform westward stress is applied (southern hemisphere). The downwelling, which produces the bottom water, and upwelling are much stronger when the wind is blowing. (Compare the left-hand side of figure 22*a* (ii) with figure 21*c*.)

A uniform grid with 18 points in the vertical was used. The assumptions listed at the beginning of §3 were made and eddy diffusivities were the same as eddy viscosities. The ratio of the lateral viscosity A and vertical viscosity ν was made equal to the square $(L/H)^2$ of the aspect ratio, H being depth and L the width at the bottom. The thermal Rossby number, B/Af^2, was 0.2, where $B = \nu g \max(-\rho_z)_{\text{surface}}/\rho$ is the maximum surface buoyancy flux and f the Coriolis parameter. The ratio, $f\tau L/BH$, of wind to buoyancy forcing was 40, τ being the surface stress and the Ekman number ν/fH^2 was 10^{-3}.

into equilibrium. Another project will take on added significance if the first is successful. This aims at calculating the distribution of tracers given the velocity field. In both cases the results depend on assumptions about eddy viscosities or eddy diffusivities, but one can vary these in order to find a best fit to data and so by comparing models and observation find out something about the ocean. (Kuo & Veronis (1970) have used this technique for a simple model of the abyssal circulation.)

3.5. *Problems of resolution and computer time*

Now, to keep things in perspective, I would like to discuss some of the problems inherent in making these three-dimensional models. There are basically three problems—one of resolution which really depends on availability of storage space on the computer: one of the computer time per calculation—this is related to the resolution problem as well as to the speed of computers—and thirdly, the dynamical one of whether the treatment of Reynolds stresses and heat fluxes through eddy viscosity and eddy diffusivity parameters is satisfactory or not.

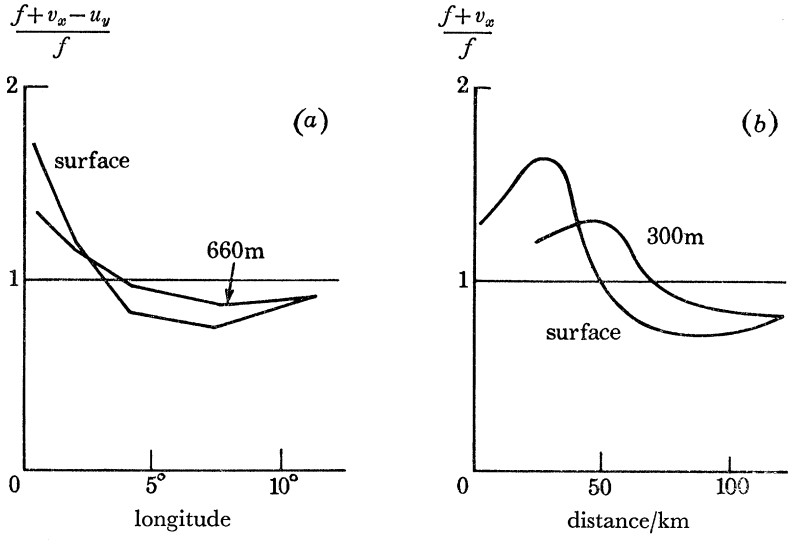

FIGURE 23. Ratio of the vertical component, $f+v_x-u_y$, of the total vorticity to the vertical component, f, of the planetary vorticity for: (*a*) a numerical model (Gill & Bryan 1971, case 15-I, at 31° latitude); (*b*) the Gulf Stream at 33° N (see figure 5). In the numerical case, the rotation of the Earth was reduced by a factor of 10 in order to give a wide nonlinear boundary layer. Comparison with observation shows the model boundary layer is wider and deeper than the observed layer, but has a similar profile and is nonlinear to a similar degree. In the model, the western wall was vertical and the depth was 4000 m.

Let us begin by discussing *horizontal resolution*. Even if we forget about upwelling layers, it can be seen from figure 5 that resolution of the Gulf Stream requires a horizontal grid spacing of 20 km (or less). A uniform net of this spacing would require about 100 000 grid points per grid level to cover just the North Atlantic Ocean. This is over 100 times the number that has been found feasible to date, so clearly special measures have to be taken. One can improve things by using grids with extra resolution near the boundaries, but this is only a partial help. Therefore one has to compromise with values of the parameters to make the western boundary current thicker. This can be done by using very large values of the lateral eddy viscosity. This not only thickens the western boundary layer but also makes it linear. To make the boundary layer nonlinear as well requires a reduction in the rate of the rotation of the Earth. The effect of such changes is illustrated in figure 23. The model boundary layer is thicker and deeper than the observed Gulf Stream, but has a similar profile and is nonlinear to a similar degree. Thus models can produce good qualitative agreement with observation, and quantitative comparison can only be made on the basis of scaling assumptions. It is, however, difficult to do this in a model with a large number of parameters and a rather complex structure (see figure 13).

The resolution problem would be made worse if it were found that eddy processes with the

Gulf Stream scale must be included to properly represent ocean dynamics, for then a 20 km spacing would perhaps be needed for the whole ocean basin and not just in the boundary region. In atmospheric models it has been found essential to include eddy processes but the scale of the significant eddies is such that a grid spacing of about 250 km seems to be sufficient.

Computer time. The difficulty here is due to the large disparity between the time step needed for computational stability—typically an hour or so and the length of time needed for the density field to reach equilibrium—typically of the order of centuries. Thus the number of time steps involved is often of the order of 100 000 and typically 1 week's computer time is required for each calculation. This is so large that the number of calculations that can be made is severely restricted.

Vertical resolution. Some criticisms have been made of the lack of resolution of the surface Ekman layer in these models, for, except near the equator, the upper layer of the model (usually about 50 m thick) is thicker than the Ekman layer. However, the finite difference equations are so written that the Ekman fluxes and Ekman divergence have the values that theory requires (see Appendix to Bryan & Cox 1968*a*) so that the effect of the Ekman divergence on the rest of the ocean is correctly modelled. Also, the upper layer of more recent models is treated as a mixed layer (temperature and salinity independent of depth), as it is generally observed to be. Accordingly, the heat fluxes of the layer and the heat transfer to the rest of the ocean is correctly represented (appendix to Bryan & Cox 1968*a*).

Improvements in the way the upper layer is treated would require a better understanding of the mixed layer than we now have. Most progress has so far come from studying time-varying transfers of momentum and heat, as these tend to be larger than the mean transfers. Pollard & Millard's (1970) model shows that *momentum* is continually transferred across the sea surface into and out of the mixed layer, the change mainly being at near-inertial frequencies. The transfers, at these frequencies, of momentum from the mixed layer to the ocean below are much smaller than the transfers across the sea surface, so the mixed layer can be regarded as a buffer zone which 'protects' the deep ocean from some of the variability imposed at the surface. Models of the mixed layer involving the *heat* transfer to and from the layer have been developed by Turner & Kraus (1967) and Kraus & Turner (1967). It is a matter of observation that much of the heat transferred across the surface into the mixed layer is not transferred to the deep ocean, so that the mixed layer is a buffer zone for heat transfer as well as momentum transfer. The existence of the buffer implies that, for studies of the deep ocean, it is not necessary to know full details of the transfer processes at the surface as a function of time, more limited information being sufficient. On the other hand, for certain air–sea interaction processes, details of the behaviour of the mixed layer may be vital, while the response of the deep ocean may be less important.

3.6. *The role of eddy processes*

As with all turbulent flow problems (cf. Kline, Moffatt & Morkovin 1969), there is a problem of how to treat eddy processes. In the models, these have so far been represented by means of eddy viscosity and eddy diffusivity coefficients, but is this form of representation appropriate? (See Stommel 1970.) Processes that are represented through eddy viscosity coefficients can in a steady-state model, only lead to removal of energy from the mean flow, but Webster's (1965) measurements (figure 6) indicate that energy is actually transferred *to* the mean flow by eddies on the inner side of the Gulf Stream. This, of course, is a very special region, but the measurements point to the *possibility* that eddies may play a similar role in other parts of the ocean.

Let us consider three ways in which eddies may be generated, and how they might arise in

models. The first way is through an instability of the mean flow itself. In this case, the eddies would be expected to appear spontaneously in a time-dependent calculation, so that the model circulation would never settle down to a steady state. This actually happens in some models (Bryan & Cox 1968*b*; Gill & Bryan 1971). However, instabilities on a scale that can not be resolved by the grid will not arise, nor will small-scale instabilities occur if the friction coefficients are set too high. Also the stability characteristics of the rather spread out boundary layers of the models may be different from those of the more intense layers observed. In other words, the compromises associated with resolution problems may prevent the spontaneous appearances of eddies. Examples of eddies that are thought to arise spontaneously (Orlanski 1969; Robinson & Gadgil 1970) are the Gulf Stream eddies discussed by Professor Robinson (1971) in the first paper of the meeting. These eddies may play an important role in removing vorticity put into the ocean elsewhere by the wind stress.

A second mechanism is by interaction of the mean flow with bottom topography. The eddies generated in this way would also arise naturally in a calculation if the appropriate eddy scales and topography scales are sufficiently well resolved. In the models I have discussed, topographic effects were not included. (A cine film which demonstrated this interaction of mean flow and topography for a homogeneous model was shown at the meeting by Dr P. B. Rhines.)

A third mechanism is through time-dependent forcing at the surface. Disturbances of this type were discussed by Professor Lighthill (1971) in the preceding paper. Veronis (1970) has studied numerically effects of such forced fluctuations on the mean flow in a two-dimensional model, following an analytic study of Pedlosky (1965) and concluded that they can significantly increase the mass transport of the Gulf Stream. The Medoc group (1970) has shown that seasonal effects are important for bottom water formation in the Mediterranean. It would thus be essential to include seasonal variations in models to reproduce effects of this type. Dr Swallow (1971) will be discussing later in the meeting a type of eddy which could play an important part in the circulation, but the mode of generation of these eddies has not yet been identified.

The three mechanisms suggested above are not necessarily (or even likely to be) independent of each other, but models could be designed to include all three effects. However, resolution problems clearly impose severe restrictions on our potential ability to correct model observed currents and their fluctuations, because of the great range of scales involved.

In conclusion, I would like to mention three ways in which models can be used in future:

(i) Continued attempts should be made using eddy viscosity and eddy diffusivity coefficients to see how well such models can approximate to observation. Such models have already shown a capability to reproduce well major features of the circulation, and there is no reason to believe they cannot be improved further.

(ii) Special models, like that discussed by Professor Robinson (1971), or that of Killworth (figure 22), are invaluable in improving understanding of detailed processes which are relatively local in nature.

(iii) Models deliberately designed to investigate time-dependent processes in relation to the mean flow will help our understanding of this aspect of the circulation. There is a need for more studies, both analytic and numerical, in which effects of stratification and bottom topography are included.

Finally, of course, there must be a continuous interaction between model studies and observation. On the one hand, model studies are motivated by a desire to understand observed features of the ocean. On the other hand, observations are required to test ideas that arise from model

PHILOSOPHICAL TRANSACTIONS OF THE ROYAL SOCIETY A MATHEMATICAL, PHYSICAL & ENGINEERING SCIENCES

studies. If you like, improvements in our understanding of the ocean depend on our ability to design good observational experiments, our ability to design good models and our ability to relate the observations and the models.

References (Gill)

Baker, D. J. 1971 *Geophys. Fl. Dyn.* **2**, 17.
Baker, D. J. & Robinson, A. R. 1969 *Phil. Trans. R. Soc. Lond.* A **265**, 533.
Beardsley, R. C. 1969 *J. Fluid Mech.* **38**, 255.
Bryan, K. 1963 *J. atmos. Sci.* **20**, 594.
Bryan, K. 1969 *J. comp. Phys.* **4**, 347.
Bryan, K. & Cox, M. D. 1967 *Tellus* **19**, 54.
Bryan, K. & Cox, M. D. 1968*a* *J. atmos. Sci.* **25**, 945.
Bryan, K. & Cox, M. D. 1968*b* *J. atmos. Sci.* **25**, 968.
Charney, J. G. 1955 *Proc. natn. Acad. Sci., U.S.A.* **41**, 731.
Charney, J. G. 1960 *Deep Sea Res.* **6**, 303.
Cox, M. D. 1970 *Deep Sea Res.* **17**, 47.
Ekman, F. W. 1905 *Ark. Mat., Astr. Fys.* **17**, no. 26.
Gill, A. E. 1968 *J. Fluid Mech.* **32**, 465.
Gill, A. E. 1971 *Deep Sea Res.* **18**, 421.
Gill, A. E. & Bryan, K. 1971 *Deep Sea Res.* **18**, 685.
Hellerman, S. 1965 *Mon. Weath. Rev.* **93**, 239.
Hellerman, S. 1967, 1968 *Mon. Weath. Rev.* **95**, 607. (Corrected tables, **96**, 63.)
Hicks, B. B. & Dyer, A. J. 1970 *Q. Jl R. met. Soc.* **96**, 523.
Hidaka, K. 1954 *Trans. Am. geophys. Un.* **35**, 431.
Hidaka, K. 1958 *Rec. oceanogr. Wks, Japan* **4** (2), 77.
Ilyin, A. M., Kamenkovich, V. M., Zhugrina, T. G. & Silkina, M. M. 1969 *Izv., atmos. & Ocean. Phys.* **5**, 1160. (Engl. transl. p. 668.)
Kendall, R. T. 1970 Ph.D. Thesis, Nova University.
Kline, S. J., Moffatt, H. K. & Morkovin, M. V. 1969 *J. Fluid Mech.* **36**, 481.
Knauss, J. A. 1966 *J. mar. Res.* **24**, 205.
Knauss, J. A. 1970 *Deep Sea Res.* (suppl. to **16**), 117.
Kraus, E. B. & Turner, J. S. 1967 *Tellus* **19**, 98.
Kuo, H.-H. & Veronis, G. 1970 *Deep Sea Res.* **17**, 29.
Lighthill, M. J. 1971 *Phil. Trans. R. Soc. Lond.* A **270**, 371. (This volume.)
Matthäus, W. 1969 *Beitr. Meereskunde* **23**, 37.
McKee, W. D. 1970 Ph.D. Thesis, University of Cambridge.
Medoc group 1970 *Nature, Lond.* **227**, 1037.
Miyake, M., Donelan, M., McBean, G., Paulson, C., Badgley, F. & Leavitt, E. 1970 *Q. Jl R. met Soc.* **96**, 132.
Morgan, G. W. 1956 *Tellus* **8**, 301.
Munk, W. H. 1950 *J. Met.* **7**, 79.
Munk, W. H. 1966 *Deep Sea Res.* **13**, 707.
Niiler, P. P. 1966 *Deep Sea Res.* **13**, 597.
Orlanski, I. 1969 *J. atmos. Sci.* **26**, 1216.
Ozmidov, R. V., Belyayev, V. S. & Yampolskiy, A. D. 1970 *Izv., atmos. Ocean. Phys.* **6**, 285. (Engl. transl. p. 160.)
Pak, H., Beardsley, G. F. & Smith, R. L. 1970 *J. geophys. Res.* **75**, 629.
Pedlosky, J. 1965 *J. atmos. Sci.* **22**, 267.
Pedlosky, J. 1968 *J. Fluid Mech.* **32**, 809.
Pollard, R. T. & Millard, R. C. 1970 *Deep Sea Res.* **17**, 813.
Reid, J. L. 1965 *Intermediate waters of the Pacific Ocean.* Johns Hopkins Oceanographic Studies, vol. 2.
Richardson, W. S., Schmitz, W. J. & Niiler, P. P. 1969 *Deep Sea Res.* (suppl. to **16**), 225.
Robinson, A. R. (ed.) 1963 *Wind-driven ocean circulation: a collection of theoretical studies.* New York, London: Blaisdell.
Robinson, A. R. 1966 *J. mar. Res.* **24**, 179.
Robinson, A. R. 1971 *Phil. Trans. R. Soc. Lond.* A **270**, 351. (This volume.)
Robinson, A. R. & Gadgil, S. 1970 *Geophys. Fl. Dyn.* **1**, 411.
Sarkisyan, A. S. 1966 *Theory and computation of Ocean currents.* Gidrometeoizdat. (English translation IPST Press, Jerusalem 1969, available from U.S. Dep. of Commerce, Springfield, Virginia.)
Sarkisyan, A. S. 1969 *Izv., Atmos. & Ocean. Phys.* **5**, 818. (Engl. transl. p. 466.)
Sarkisyan, A. S. & Pastukhov, A. F. 1970 *Izv., Atmos. & Ocean. Phys.* **6**, 64. (Engl. trans. p. 34.)
Schmitz, W. J. & Niiler, P. P. 1969 *Tellus* **21**, 814.
Smith, R. L., Pattullo, J. G. & Lane, R. K. 1966 *J. geophys. Res.* **71**, 1135.

PHILOSOPHICAL TRANSACTIONS OF THE ROYAL SOCIETY A MATHEMATICAL, PHYSICAL & ENGINEERING SCIENCES

Smith, S. S. 1970 *J. geophys. Res.* **75**, 6758.
Stommel, H. 1948 *Trans. Am. geophys. Un.* **29**, 202.
Stommel, H. 1957 *Deep Sea Res.* **4**, 149.
Stommel, H. 1958 *Deep Sea Res.* **5**, 80.
Stommel, H. 1960 *Deep Sea Res.* **6**, 298.
Stommel, H. 1965 *The Gulf Stream* (2nd ed.). Berkeley and Los Angeles: University of California Press; Cambridge University Press.
Stommel, H. 1970 *Science, N.Y.* **168**, 1531.
Stommel, H. & Arons, A. B. 1959 *Deep Sea Res.* **6**, 140.
Stommel, H. & Arons, A. B. 1960 *Deep Sea Res.* **6**, 217.
Stommel, H., Arons, A. B. & Faller, A. J. 1958 *Tellus* **10**, 179.
Sverdrup, H. U. 1947 *Proc. Natn. Acad. Sci. U.S.A.* **33**, 318.
Swallow, J. C. 1971 *Phil. Trans. R. Soc. Lond.* A **270**, 451. (This volume.)
Swallow, J. C. & Worthington, L. V. 1961 *Deep Sea Res.* **8**, 1.
Takano, K. 1969 *J. oceanog. Soc. Japan* **25** (1), 48.
Turner, J. S. & Kraus, E. B. 1967 *Tellus* **19**, 88.
Veronis, G. 1966 *Deep Sea Res.* **13**, 31.
Veronis, G. 1970 *Deep Sea Res.* **17**, 421.
Von Arx, W. S. 1952 *Tellus* **4**, 311.
Warren, B. A. 1971 *Nature Phys. Sci.* **229**, 18.
Warren, B. A., Stommel, H. & Swallow, J. L. 1966 *Deep Sea Res.* **13**, 825.
Warren, B. A. & Voorhis, A. D. 1970 *Nature, Lond.* **228**, 849.
Webster, F. 1965 *Tellus* **17**, 239.
Welander, P. 1971 *Phil. Trans. R. Soc. Lond.* A **270**, 415. (This volume.)
Wooster, W. S. & Jones, J. H. 1970 *J. mar. Res.* **28**, 235.
Wooster, W. S. & Reid, J. L. 1963 *Eastern boundary currents in the Sea* (vol. 2, M. N. Hill, general editor). New York, London: Interscience.
Wyrtki, K. 1963 *Bull. Scripps. Instn Oceanogr.* **8**, 313.

PHILOSOPHICAL TRANSACTIONS OF THE ROYAL SOCIETY A MATHEMATICAL, PHYSICAL & ENGINEERING SCIENCES

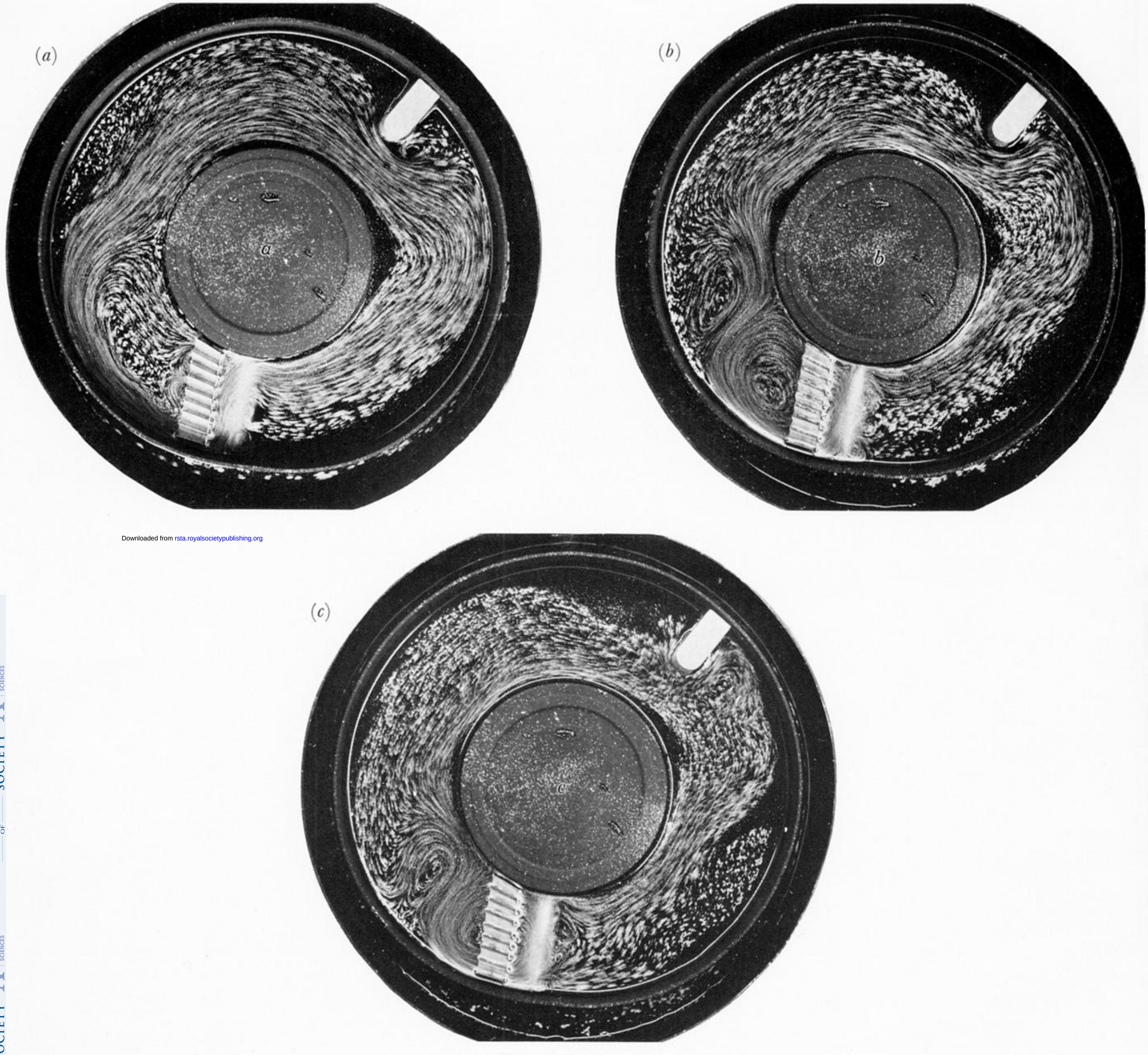

FIGURE 9. Experimental results of J. W. Elder (private communication) showing the effect of variation of β on currents through a model Drake Passage, which is at the top right of each picture. A thin layer (about 1 cm) of fluid is driven clockwise by an impellar which is seen (at the bottom of each picture). The β effect is provided by the free surface curvature which is produced by the rotation, and increases from (*a*) to (*c*). As β increases, so does the asymmetry of the motion through the gap, a western boundary current (corresponding to the Falkland current) being well-established in case (*c*).